



Enhancing visible light photocatalytic activity of TiO₂ using a colorless molecule (2-methoxyethanol) due to hydrogen bond effect

Zaiyong Jiang^a, Yuanyuan Liu^{a,*}, Tao Jing^b, Baibiao Huang^{a,*}, Zeyan Wang^a, Xiaoyang Zhang^a, Xiaoyan Qin^a, Ying Dai^b

^a State key Laboratory of Crystal Materials, Shandong University, Jinan 250100, PR China

^b School of Physics, Shandong University, Jinan 250100, PR China

ARTICLE INFO

Article history:

Received 7 January 2016

Received in revised form 28 May 2016

Accepted 14 July 2016

Available online 15 July 2016

ABSTRACT

Extending the light absorption of TiO₂ to the visible region is realized using a colorless molecule (2-methoxyethanol). The as-prepared MES-TiO₂ displays efficient photocatalytic activity under visible light irradiation. The hydrogen bond between MES and TiO₂ is found to be responsible for the visible light absorption of TiO₂, which is confirmed by FT-IR, DRS, PL spectra and density of states calculation.

© 2016 Elsevier B.V. All rights reserved.

Keywords:

TiO₂

Photocatalyst

Degradation

Hydrogen bond

1. Introduction

Since the discovery of photocatalytic water splitting on TiO₂ electrode by Honda et al. in 1972 [1], TiO₂ is widely used in renewable energy substitutes and environmental decontamination, due to its low cost, chemical stability, nontoxic and environmental friendly features, etc [2–5]. However, the band gap of TiO₂ is wide (3.2 eV in the anatase phase), which means TiO₂ is only active in the ultraviolet (UV) region [6–8]. This fact critically limits further practical application of TiO₂ as UV light accounts for 4.7% of solar energy. In order to take full advantage of the solar energy, it is necessary to expand the absorption of TiO₂ into visible region.

Over the past few years, various efficient methods were proposed, such as doping TiO₂ with metal or nonmetal elements [9–12], self-doped Ti³⁺ in TiO_{2-x} [13–15], dye sensitization [16] and fabrication of TiO₂ based organic-inorganic hybrid materials [17–21] etc. Among them, the fabrication of TiO₂-based organic-inorganic hybrid materials attracted increasing attention and was considered as a promising strategy for achieving effective visible light harvest. Prof. Ye et al. prepared yellow TiO₂ nanocrystals via compositing benzyl alcohol with TiO₂ gels. They thought it was the interfacial Ti–Ti bonding that was responsible for greatly enhanced visible light absorption [17]. Prof. Yamashita et al.

assembled organic dyes with TiO₂, and through sensitizing effect, TiO₂ exhibited efficient activity under visible light irradiation [22]. Prof. Berenguer synthesized mesoporous organo-titanias using the colored (4,6-dihydroxypyrimidine and *p*-phenylenediamine). The mesoporous organo-titanias display a decreased band gap (3.17 eV and 2.74 eV) due to the combined effect of doping of organic component and Ti(IV) partial reduction [18]. Prof. Wonyong Choi prepared glucose adsorbed-TiO₂ nanoparticles, which showed visible photocatalytic activity through the ligand to metal charge transfer [23].

In this work, we reported an alternative way to extend the visible light absorption of TiO₂, i.e. hydrogen bonds. A novel TiO₂-based organic-inorganic hybrid material was prepared via one-pot facile solvothermal method using the colourless organic molecule (2-methoxyethanol, MES). The as-prepared MES-TiO₂ exhibits efficient photocatalytic activity on decomposing RhB under visible light irradiation. Rhodamine B (RhB) is one common pollutant existing in industrial waste water, which is suspected to be toxic and carcinogenic. Therefore, RhB is widely used to probe the photocatalytic performance. Further investigation suggests that the interaction between MES and TiO₂ is hydrogen bonds, i.e. O of CH₃—O in MES and H atom of hydroxyl on the surface TiO₂. It is the hydroxyl bond that is responsible for the visible light absorption of MES-TiO₂.

* Corresponding authors.

E-mail addresses: yliu@sdu.edu.cn (Y. Liu), bbhuang@sdu.edu.cn (B. Huang).

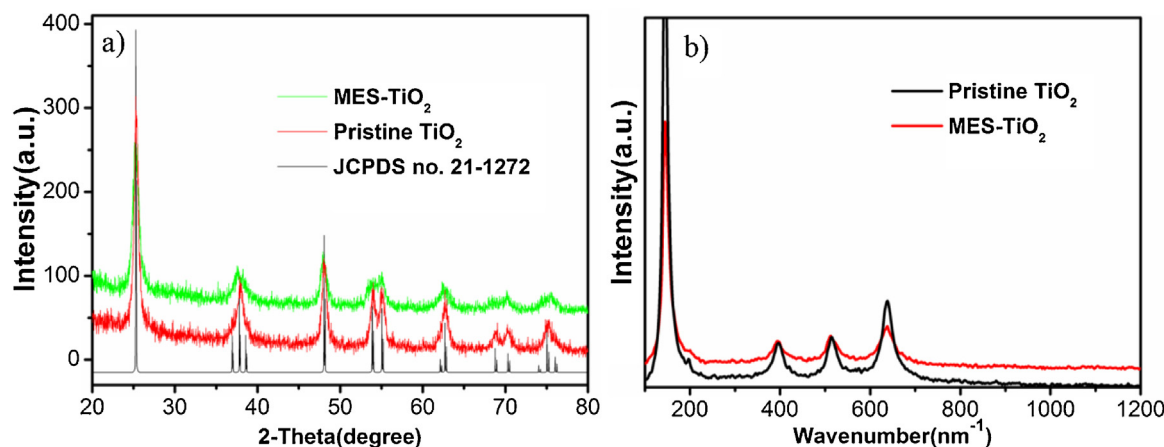


Fig. 1. XRD patterns (a) and Raman spectra (b) of pristine TiO₂ and MES-TiO₂.

2. Experimental

2.1. Synthetic procedure

MES-TiO₂ nanocomposite was synthesized via a one-pot solvothermal method. Firstly, 30 ml ethanol and 20 ml 2-methoxyethanol (MES) were mixed together under vigorous stirring. After that, 2 ml of deionized water was added into above solution with stirring. Finally, 1 ml tetrabutyl titanate was dropped into the mixed solution and steadily stirred 20 min. After that, the solution was transferred into a 100 ml autoclave, and kept at 180 °C for 24 h. After being cooled down to room temperature, the as-prepared sample was washed several times with deionized water and ethanol, which was dried in a vacuum oven at 60 °C for 6 h. Moreover, the pristine TiO₂ is prepared using 50 ml ethanol without any MES under the same condition described above. For comparison, the MES-TiO₂ was milled using the agate mortar to obtain the “Milled MES-TiO₂” sample. The photo-physical and photocatalytic properties of the Milled MES-TiO₂ were investigated, and the results confirmed the proposed mechanism of visible light induced photocatalytic activity of the Milled MES-TiO₂.

2.2. Characterization

Powder X-ray diffraction (XRD) patterns were obtained on a Bruker AXS D8 advance powder diffractometer with Cu K α X-ray radiation. Raman spectra were carried out by using Horiba LabRAM HR system with laser radiation ($\lambda=1064$ nm) used as excitation source. The infrared (IR) spectra were characterized by using a Fourier transform infrared spectrometer. The XPS was analyzed using a Thermo Fisher Scientific (ESCALAB 250) X-ray photoelectron spectrometer, which was charge corrected to the adventitious C 1 s peak at 284.8 eV. Scanning electron microscope (SEM) images were obtained via the Hitachi S-4800 microscope. Transmission electron microscope (TEM) and high-resolution transmission electron microscopy (HRTEM) measurements were performed on a JEOL-2100 microscope. UV-vis diffuse reflection images were obtained by using a Shimadzu UV 2550 recording spectrophotometer, which was equipped with an integrating sphere.

2.3. Photocatalytic activity studies

The photocatalytic activities of as-prepared samples were investigated via degrading the RhB solution (20 mg/L). 0.1 g of photocatalyst was added into 100 ml RhB solution with stirring, which was kept in the dark for 2 h in order to obtain the equilibrium adsorption state. A 300 W Xe arc lamp (PLS-SXE300, Beijing Trust-

tech Co. Ltd) with an ultraviolet cutoff filter was used as the light source so as to provide visible light with $\lambda>420$ nm. At the given time interval, the aqueous solution was withdrawn and monitored by UV/Vis spectroscopy (UV-7502PC, Xinmao, Shanghai).

2.4. Computational method

Our theoretical calculations are based on the density functional theory as implemented in the Vienna ab initio simulation package (VASP). The generalized gradient approximation (GGA) in the formulation of Perdew-Burke-Ernzerhof (PBE) was employed for exchange-correlation functional. The cutoff energy for the wavefunction expansion is 400 eV. The energy convergence criterion was 10⁻⁵ eV and the Hellmann-Feynman forces were relaxed to less than 0.03 eV Å⁻¹. To simulate the organic glycol adsorbed on the surface of TiO₂, the (101) surfaces are constructed by the stoichiometric (4 × 3) slab models consisting of 9 atomic layers (216 atoms). K-point sampling is performed using the Monkhorst-Pack scheme, with a (1 × 1 × 1) sampling grid. In the case of slabs, a 18 Å thickness of the vacuum layer is used to avoid the interaction between repeated slabs. An extra Hydrogen atom is added to the surface to maintain charge balance of OH adsorbed TiO₂ (101) surface. Before the absorption, the OH adsorbed TiO₂ (101) surface and organic glycol are calculated in the same periodic supercell. The organic glycol is positioned in a number of configurations at the surface and a full relaxation is performed within a fixed supercell.

3. Results and discussion

3.1. Structure and morphology

The crystal structures of as-prepared samples were characterized by XRD and Raman spectra. Fig. 1a displays the XRD patterns of pristine TiO₂ and MES-TiO₂. All the diffraction peaks for the two samples could perfectly match with the characteristic diffraction of anatase TiO₂ (JCPDS no. 21-1272). Compared with pristine TiO₂, the diffraction intensity of MES-TiO₂ is weaker, and the diffraction shape is broader, suggesting a reduction in the crystallinity, which is likely to be caused by the introduction of MES. Analysis of Raman spectra (Fig. 1b) further supports the XRD results. Both pristine TiO₂ and MES-TiO₂ exhibit typical anatase Raman bands. The peaks at 144, 197, 396, 513 and 639 cm⁻¹ are ascribed to the E_g, E_g, B_{1g}, A_{1g} and E_g modes of anatase phase of TiO₂, respectively [24,25]. In addition, the full width at half maximum (FWHM) of MES-TiO₂ is larger than that of pristine TiO₂, implying various defects or local disorder of MES-TiO₂ [24,25].

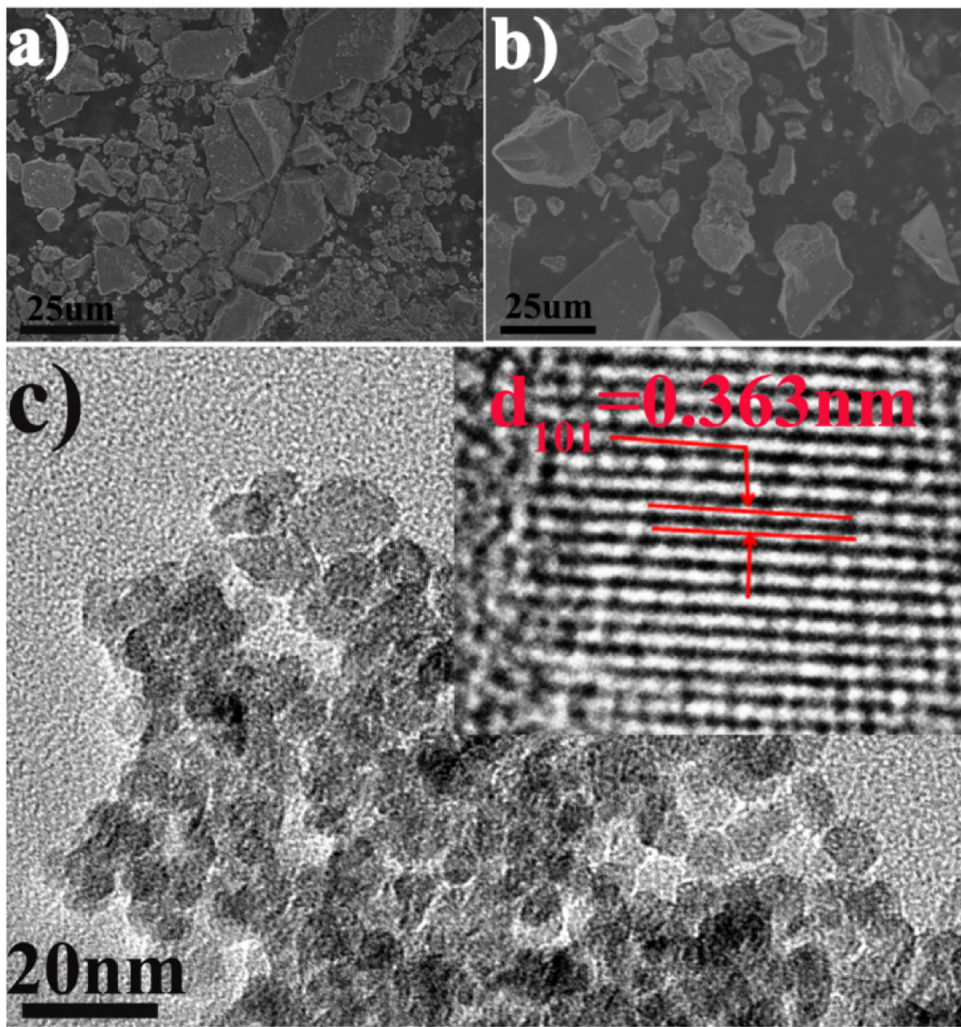


Fig. 2. SEM images of pristine TiO₂ (a) and MES-TiO₂ (b), HRTEM image of MES-TiO₂ (c).

The SEM images suggest that both samples possess irregular block morphology (Fig. 2a–b). No significant difference between pristine TiO₂ and MES-TiO₂ is observed. HRTEM images (Fig. 2c) suggest that the irregular block consists of some MES-TiO₂ nanoparticles with the average particle size of about 7 nm. The measured lattice spacing of 0.363 nm is close to the d-spacing of 101 plane of anatase TiO₂.

3.2. Characterization of samples by UV-vis spectroscopy

Fig. 3a exhibits the DRS pristine of TiO₂ and MES-TiO₂. It is obvious that the absorption band edge of MES-TiO₂ is red shifted to 605 nm, compared to that of pristine TiO₂ (406 nm). This result is consistent with the color of the sample, i.e. from white to deep yellow after the introduction of MES (inset of Fig. 3a). This result clearly indicates that the introduction of MES extends the absorption of TiO₂ from UV to visible light region. In addition, the band gap of MES-TiO₂ is further determined to be 2.10 eV (Fig. 3b), about 0.96 eV lower than that of pristine TiO₂ (3.06 eV).

3.3. Photocatalytic activity

The visible light photocatalytic activity of MES-TiO₂ was evaluated using RhB as a target molecule. For comparison, the photocatalytic activity of pristine TiO₂ was also carried out under

the same conditions. The results are displayed in Fig. 4. It can be obviously observed that MES-TiO₂ exhibits much better degradation efficiency than pristine TiO₂. After 150 min irradiation, about 99.5% percent of RhB molecules are decolorized over MES-TiO₂, while only 34.1% percent are decolorized over TiO₂. In order to eliminate the effect of dye sensitization and determine the effective visible photocatalytic performance of MES-TiO₂, the colorless phenol (20 mg/L) was chosen as a target molecule under visible light irradiation. Approximate 60% phenol molecules were removed after 8 h visible light irradiation, indicating that MES-TiO₂ indeed displays visible photocatalytic activity.

3.4. Characterization of samples by XPS and EPR

In order to explore the origin of visible light absorption of MES-TiO₂, XPS spectrum of MES-TiO₂ was investigated. As shown in Fig. 5, two strong peaks of Ti 2p spectra at 458.73 eV and 464.58 eV are detected (Fig. 5a), which are assigned to Ti⁴⁺ 2P_{3/2} and Ti⁴⁺ 2P_{1/2}, respectively. No peak assigned to Ti³⁺ (Ti³⁺ 2P_{3/2} at 457.31 eV, Ti³⁺ 2P_{1/2} at 461.12 eV) [26] can be fitted. Furthermore, there are two peaks locating at 530.02, 531.41 eV (Fig. 5b), which are assigned to the lattice oxygen and hydroxyl groups of MES-TiO₂, respectively. It is noteworthy to point out that no peak assigned to oxygen vacancies (at 532.8 eV) was detected and fitted (Fig. 5b) [24,27]. Moreover, in order to further confirm the absence of Ti³⁺ or oxy-

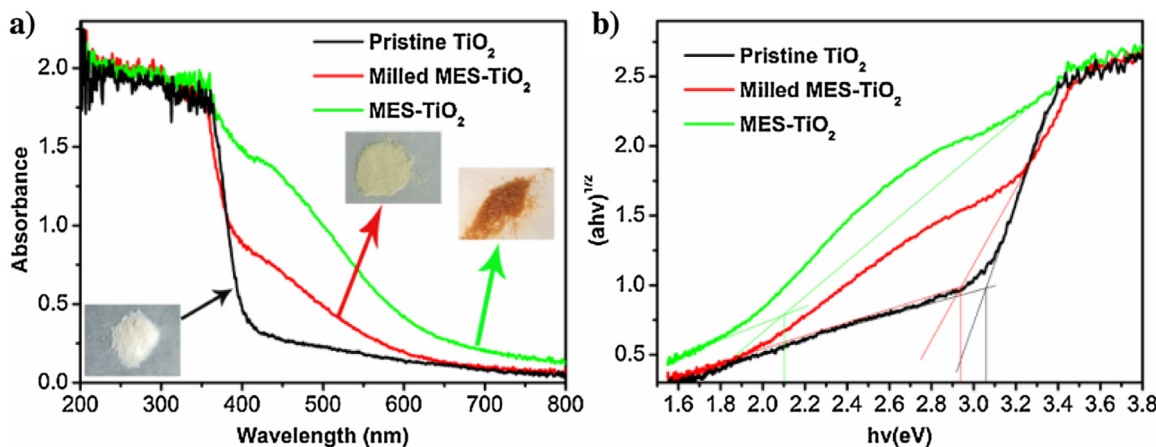


Fig. 3. (a) UV-vis DRS spectra of pristine TiO₂, Milled MES-TiO₂ and MES-TiO₂ and (b) plots of $(ahv)^{1/2}$ versus the photon energy (hv).

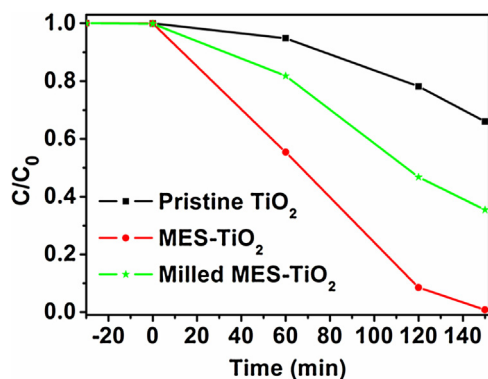


Fig. 4. Photocatalytic degradation of RhB over pristine TiO₂, Milled MES-TiO₂ and MES-TiO₂, respectively.

gen vacancies, EPR spectra were further performed and the results were shown in Fig. 5c. No EPR signals of MES-TiO₂ ascribed to Ti³⁺ (characteristic signal at a g value of 1.97) or oxygen vacancies (characteristic signal at a g value of 2.0036) were detected under our experimental conditions [25,27]. The above results suggest that the visible light absorption of MES-TiO₂ is not caused by Ti³⁺ or oxygen vacancies.

3.5. FT-IR spectra

FT-IR spectrum was carried out in order to investigate the interaction between MES and TiO₂, and further explore the origin of visible light absorption of MES-TiO₂. For comparison, the FT-IR spectra of pristine TiO₂ and MES were also performed. As shown in Fig. 6, most characteristic peaks of the MES are found in the MES-TiO₂, which suggests the presence of MES onto TiO₂. Three vibrational peaks at 827, 895 and 965 cm⁻¹ related to –OH groups of MES disappear in the MES-TiO₂ [28], indicating that MES are chemically adsorbed onto TiO₂ via the oxygen of –OH in MES. Furthermore, the vibrational peak of –OH groups of MES-TiO₂ shifts to 3215 cm⁻¹, compared to that of pristine TiO₂ (3285 cm⁻¹), which can be attributed to the formation of hydrogen bonds. Meanwhile, the peaks at 1126 cm⁻¹ (–C–O–C–) and 2823 cm⁻¹ (–CH₃) shifts to 1086 cm⁻¹ and 2872 cm⁻¹ respectively. This result further confirms the hydrogen bonds between MES and TiO₂.

3.6. Mechanism analysis

It is well known that the hydrogen bond can be destroyed by mechanical force. Therefore, the MES-TiO₂ was milled using the agate mortar. As can be seen from Fig. 6, the FT-IR spectrum of Milled MES-TiO₂ displays similar peaks to pristine TiO₂, and the characteristic peaks intensity of MES become very weak, suggesting the broken of hydrogen bond between MES and TiO₂. After milling, the deep yellow color of MES-TiO₂ becomes very shallow and the absorption band edge is obviously blue shifted compared to those of MES-TiO₂ without milling (Fig. 3a). In addition, the photocatalytic activity of Milled MES-TiO₂ decreases (Fig. 4). All these results suggest that hydrogen bond between MES and TiO₂ is likely to be responsible for the visible light absorption of MES-TiO₂.

In order to check above assumption, the first-principles calculations were performed. The relaxed structure of MES-TiO₂ was shown in Fig. 7a, we note that the O2 atom of CH₃–O–C unit in the MES molecule is bonded with the H atom of –OH on the surface of TiO₂, indicating a hydrogen bond formation between MES and TiO₂. The new formed bond length is about 1.64 Å. Based on the relaxed structure, the total density of states (DOS) and projected DOS of the MES-TiO₂ are calculated and the results are shown in Fig. 7b-d. Two impurity states can be observed from Fig. 7b in the band gap of MES-TiO₂. As can be seen in Fig. 7c, the lower impurity state is mainly composed of the 2p orbital of O2 atom of MES, while the higher one is mainly contributed by the O3 atom of MES. Moreover, a significantly hybridization between O1 and O2 atoms is observed in the lower impurity state. Due to the significant contribution of O1 atom to the lower impurity state, the electrons of O1 atom could be successfully excited to the Ti atoms, which is responsible for the visible light absorption of MES-TiO₂. H atom of the hydroxyl group on the surface of TiO₂ has no contribution to the bottom of the CB. Therefore, the electron excitation from the O2 to H of Ti-OH under the visible light is unlikely to be realized. In contrast, the O atom of the hydroxyl group has no contribution to either the valence band or the impurity state for pristine TiO₂, though lots of hydroxyl group exist on the surface of pristine TiO₂. Therefore, it is reasonable to conclude that it is the hydrogen bond between MES and TiO₂ promoted the visible light absorption of TiO₂.

Another result from the projected DOS is that the photo-generated holes can transfer through the O1–H–O2 unit and be trapped by O2 atom due to its significant larger contribution to lower the impurity state, because H atom possesses contribution to lower the impurity state (Fig. 7d). Therefore, the photo-generated

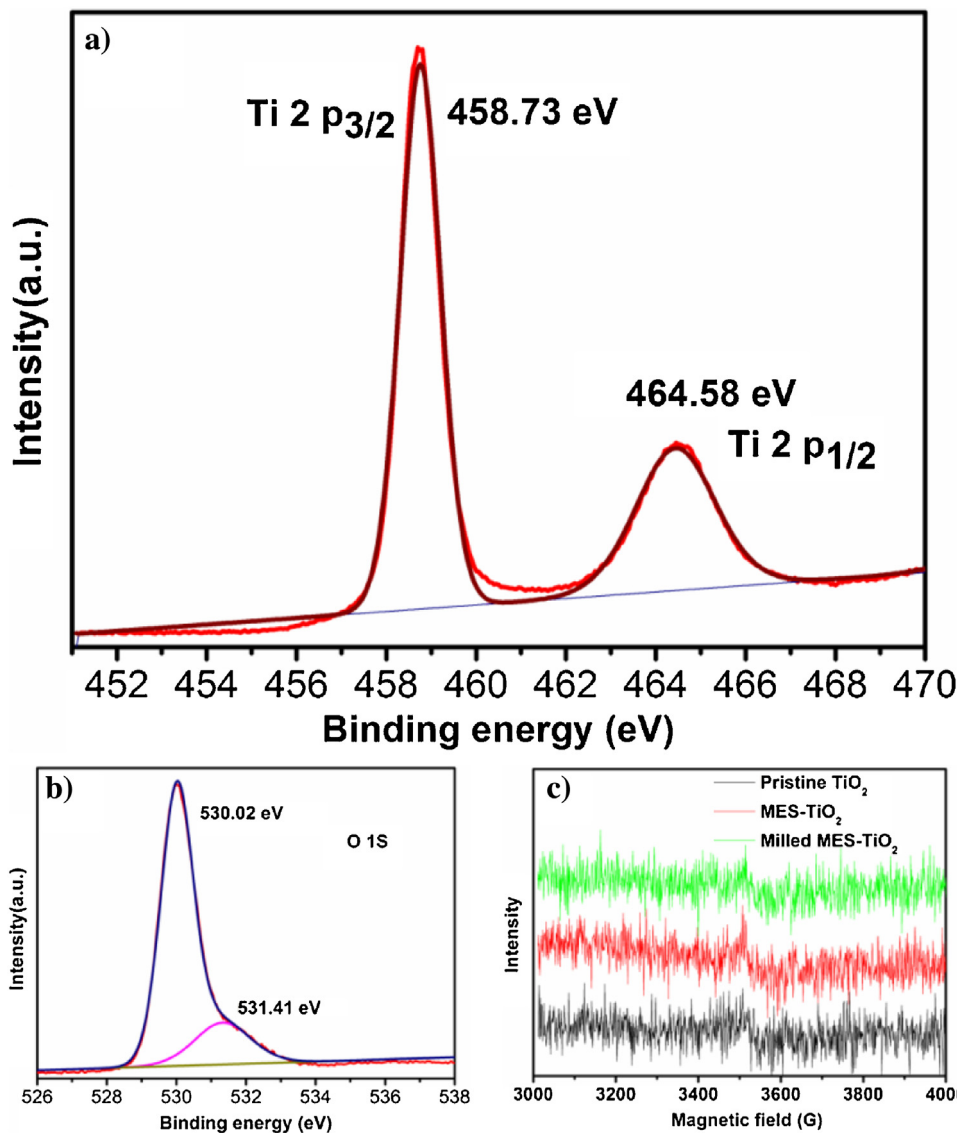


Fig. 5. XPS spectra of MES-TiO₂: (a) the Bi 4f and (b) the O 1s; (c) EPR spectra of the pristine TiO₂, Milled MES-TiO₂ and MES-TiO₂ at room temperature.

electrons and holes will be separated spatially, thereby decreasing recombination rate of carriers.

The presence of hydrogen bond between MES and TiO₂ was further proved by photoluminescence (PL) spectra. As shown in Fig. 8, the position of the emission peak of both samples was similar, but the intensity of MES-TiO₂ is obviously lower than that of pristine TiO₂. This result suggests that MES-TiO₂ possesses a much lower recombination rate of photo-generated charge carriers, compared to pristine TiO₂ [29], which is in good consistent with the DOS result. After milling (i.e. the broken of hydrogen bond between MES and TiO₂), however, the PL intensity of MES-TiO₂ decreases, suggesting the hydrogen bond plays an important role in separation efficiency of photo-generated electrons and holes. The order of PL intensity is opposite to the photocatalytic activity, which is reasonable considering the fact that PL spectrum reflects the recombination probability of photo-generated charge carriers (the larger the PL intensity, the more recombination of charge carriers).

Based on above discussion, the enhanced photocatalytic activity of MES-TiO₂ compared with that of pristine TiO₂ under visible light can be ascribed to the improvement of visible light absorption capa-

bility and the more efficient separation of photo-generated charge carrier, both of which are due to the presence of hydrogen bond.

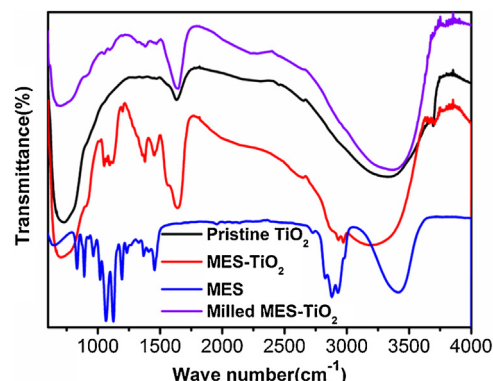


Fig. 6. FT-IR spectra of pristine TiO₂, MES-TiO₂, Milled MES-TiO₂ and MES.

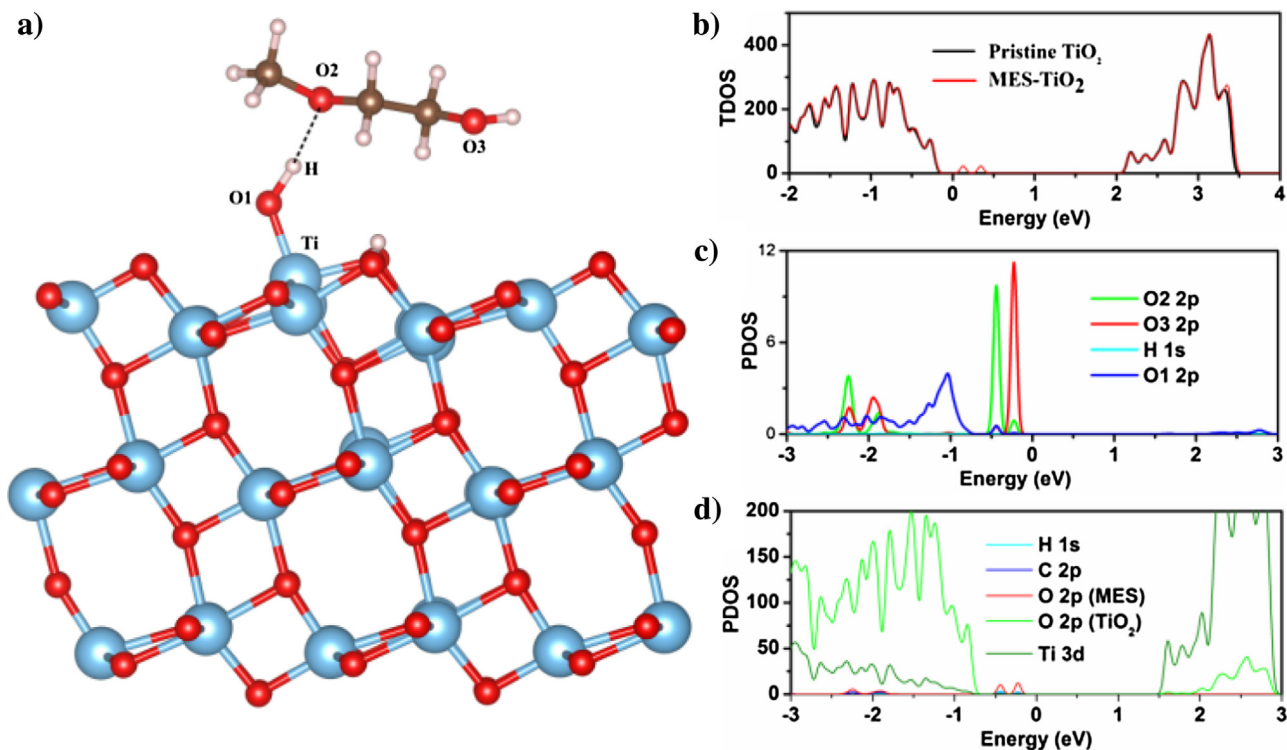


Fig. 7. The relaxed structures of MES-TiO₂ (a) and projected DOS of the MES-TiO₂ (b, c and d).

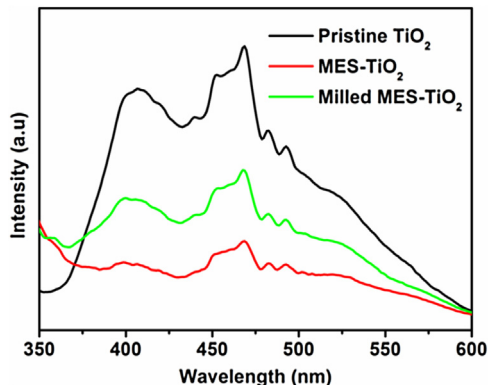


Fig. 8. PL spectra of pristine TiO₂, Milled MES-TiO₂ and MES-TiO₂.

4. Conclusions

A novel visible light responsive MES-TiO₂ (MES = 2-methoxyethanol) hybrid material was prepared via one-pot solvothermal method. MES-TiO₂ displays enhanced photocatalytic activity under visible light irradiation compared to pristine TiO₂. Density of states calculation suggests that the presence of hydrogen bond between MES and TiO₂ leads to a significantly hybridization between the O from –OH onto the surface of TiO₂ and O of CH₃–O–C– in MES, which can make the electrons of O atom from –OH onto the surface of TiO₂ be successfully excited to the surface Ti atoms so as to realize visible light absorption. Moreover, after the electron excitation, the photo-generated hole can transfer through the hydrogen bond (O–H–O unit) and be trapped by the O atom of CH₃–O–C– in MES, resulting in the effective spatial separation of photo-generated electrons and holes. This work may open a new approach to tune the optical

performances of TiO₂ with the aim of taking full advantage of the solar energy.

Acknowledgments

This work was financially supported by a research Grant from the National Basic Research Program of China (the 973 Program, No. 2013CB632401), the National Natural Science Foundation of China (No. 21573135, 21333006, 11374190, 51002091, 21007031), Taishan Scholar Foundation of Shandong Province, China and the Shandong Province Natural Science Foundation (ZR2014JL008).

References

- [1] A. Fujishima, K. Honda, *Nature* 238 (1972) 37–38.
- [2] Z. Wang, C. Yang, H. Yin, P. Chen, D. Wan, F. Xu, F. Huang, J. Lin, X. Xie, M. Jiang, *Energy Environ. Sci.* 6 (2013) 3007–3014.
- [3] Z.Y. Wang, B.B. Huang, Y. Dai, X.Y. Zhang, X.Y. Qin, Z. Li, Z.K. Zheng, H.F. Cheng, L.W. Guo, *CrystEngComm* 14 (2012) 4578–4581.
- [4] C.C. Chen, W.H. Ma, J.C. Zhao, *Chem. Soc. Rev.* 39 (2010) 4206–4219.
- [5] Y. Liu, J. Li, B. Zhou, H. Chen, Z. Wang, W. Cai, *Chem. Commun.* 47 (2011) 10314–10316.
- [6] C.T. Dinh, H. Yen, F. Kleitz, T.O. Do, *Angew. Chem. Int. Ed.* 53 (2014) 6618–6623.
- [7] A.K.P.D. Savio, J. Fletcher, K. Smith, R. Lyer, J.M. Bao, F.C.R. Hernandez, *Appl. Catal. B: Environ.* 182 (2016) 449–455.
- [8] M.Y. Wang, J. Loccozia, L. Sun, C.J. Lin, Z.Q. Lin, *Energy Environ. Sci.* 7 (2014) 2182–2202.
- [9] P. Zhang, M. Fujitsuka, T. Majima, *Appl. Catal. B: Environ.* 185 (2016) 181–188.
- [10] S.B. Rawal, H.J. Kim, W.I. Lee, *Appl. Catal. B: Environ.* 142–143 (2013) 458–464.
- [11] X.B. Chen, C. Burda, *J. Am. Chem. Soc.* 130 (2008) 5018–5019.
- [12] Y. Hu, Y.T. Cao, P.X. Wang, D.Z. Li, W. Chen, Y.H. He, X.Z. Fu, Y. Shao, Y. Zheng, *Appl. Catal. B: Environ.* 125 (2012) 294–303.
- [13] Z.K. Zheng, B.B. Huang, X.D. Meng, J.P. Wang, S.Y. Wang, Z.Z. Lou, Z.Y. Wang, X.Y. Qin, X.Y. Zhang, Y. Dai, *Chem. Commun.* 49 (2013) 868–870.
- [14] F. Zuo, L. Wang, T. Wu, Z.Y. Zhang, D. Borchardt, P.Y. Feng, *J. Am. Chem. Soc.* 132 (2010) 11856–11857.
- [15] J.C. Huo, Y.J. Hu, H. Jiang, C.Z. Li, *Nanoscale* 6 (2014) 9078–9084.
- [16] P. Giannopoulos, A. Nikolakopoulou, A.K. Andreopoulou, L. Sygellou, J.K. Hallitsis, P. Lianos, *J. Mater. Chem. A* 2 (2014) 20748–20759.
- [17] H. Tong, N. Umezawa, J.H. Ye, *Chem. Commun.* 47 (2011) 4219–4221.

- [18] M. Rico-Santacruz, A.E. Sepulveda, E. Serrano, E. Lalinde, J.R. Berenguer, J. Garcia-Martinez, *J. Mater. Chem. C* 2 (2014) 9497–9504.
- [19] J. Moon, C.Y. Yun, K.W. Chung, M.S. Kang, *J.Y. Catal. Today* 87 (2003) 77–86.
- [20] S.H. Bossmann, M. Worner, M.R. Polkherel, B. Baumeister, S. Gob, A.M. Braun, *Sep. Purif. Technol.* 67 (2009) 201–207.
- [21] M. Alvaro, E. Carbonell, V. Fornes, H. Garcia, *ChemPhysChem* 7 (2006) 200–205.
- [22] T. Kamegawa, S. Matsuura, H. Seto, H. Yamashita, *Angew. Chem. Int. Ed.* 52 (2013) 916–919.
- [23] G. Kim, S.H. Lee, W.Y. Choi, *Appl. Catal. B: Environ.* 162 (2015) 463–469.
- [24] X. Chen, P.Y. Yu, S.S. Mao, *Science* 331 (2011) 746–750.
- [25] X. Pan, M.Q. Yang, X. Fu, N. Zhang, Y.-J. Xu, *Nanoscale* 5 (2013) 3601–3614.
- [26] M.M. Khan, S.A. Ansari, D. Pradhan, M.O. Ansari, D.H. Han, J. Lee, M.H. Cho, J. *Mater. Chem. A* 2 (2014) 637–644.
- [27] Y. Yu, C.Y. Cao, H. Liu, P. Li, F.F. Wei, Y. Jiang, W.G. Song, *J. Mater. Chem. A* 2 (2014) 1677–1681.
- [28] A. Simon, L. Delmotte, J.M. Chezeau, A. Janin, J.C. Lavalle, *Phys. Chem. Chem. Phys.* 1 (1999) 1659–1664.
- [29] J. Di, J.X. Xia, S. Yin, H. Xu, L. Xu, Y.G. Xu, M.Q. He, H.M. Li, *RSC Adv.* 4 (2014) 14281–14290.